Leaf Development in the Single-Cell C_4 System in *Bienertia sinuspersici*: Expression of Genes and Peptide Levels for C_4 Metabolism in Relation to Chlorenchyma Structure under Different Light Conditions[1][OA]

María Valeria Lara, Sascha Offermann, Monica Smith, Thomas W. Okita, Carlos Santiago Andreo, and Gerald E. Edwards*

Centro de Estudios Fotosintéticos y Bioquímicos, Facultad de Ciencias Bioquímicas y Farmacéuticas, Rosario 2000, Argentina (M.V.L., C.S.A.); and School of Biological Sciences (S.O., M.S., G.E.E) and Institute of Biological Chemistry (T.W.O.), Washington State University, Pullman, Washington 99164

Bienertia sinuspersici performs C_4 photosynthesis in individual chlorenchyma cells by the development of two cytoplasmic domains (peripheral and central) with dimorphic chloroplasts, an arrangement that spatially separates the fixation of atmospheric CO_2 into C_4 acids and the donation of CO_2 from C_4 acids to Rubisco in the C_3 cycle. In association with the formation of these cytoplasmic domains during leaf maturation, developmental stages were analyzed for the expression of a number of photosynthetic genes, including Rubisco small and large subunits and key enzymes of the C_4 cycle. Early in development, Rubisco subunits and Gly decarboxylase and Ser hydroxymethyltransferase of the glycolate pathway accumulated more rapidly than enzymes associated with the C_4 cycle. The levels of pyruvate,Pi dikinase and phospho*enol*pyruvate carboxylase were especially low until spatial cytoplasmic domains developed and leaves reached maturity, indicating a developmental transition toward C_4 photosynthesis. In most cases, there was a correlation between the accumulation of mRNA transcripts and the respective peptides, indicating at least partial control of the development of photosynthesis at the transcriptional level. During growth under moderate light, when branches containing mature leaves were enclosed in darkness for 1 month, spatial domains were maintained and there was high retention of a number of photosynthetic peptides, including Rubisco subunits and pyruvate,Pi dikinase, despite a reduction in transcript levels. When plants were transferred from moderate to low light conditions for 1 month, there was a striking shift of the central cytoplasmic compartment toward the periphery of chlorenchyma cells; the mature leaves showed strong acclimation with a shade-type photosynthetic response to light while retaining C_4 features indicative of low photorespiration. These results indicate a progressive development of C_4 photosynthesis with differences in the control mechanisms for the expression of photosynthetic genes and peptide synthesis during leaf maturation and in response to light conditions.

Following the discovery of C_4 photosynthesis, the spatial compartmentation of CO_2 fixation into C_4 acids in mesophyll cells by phospho*enol*pyruvate carboxylase (PEPC) and further decarboxylation in bundle sheath cells providing Rubisco with CO_2 for fixation in the C_3 cycle were consistently linked to the occurrence of Kranz-type anatomy in terrestrial plants (Edwards and Walker, 1983; Sage and Monson, 1999). Nevertheless, three succulent species in family Chenopodiaceae, *Bienertia cycloptera*, *Bienertia sinuspersici*, and *Suaeda aralocaspica* (formerly classified as *Borszczowia*), were shown to have a unique mechanism of C_4 photosynthesis that occurs within individual photosynthetic cells (single-cell C_4 anatomy) by intracellular partitioning of enzymes and organelles (including dimorphic chloroplasts) into two compartments (Voznesenskaya et al., 2001, 2002; Edwards et al., 2004; Akhani et al., 2005). *S. aralocaspica* has a single layer of elongated, cylindrical chlorenchyma cells in which functions of C_4 photosynthesis are spatially separated to opposite ends of the cells (Voznesenskaya et al., 2003). *B. cycloptera* and *B. sinuspersici* have an unusual development of two cytoplasmic compartments in chlorenchyma cells, consisting of a large central cytoplasmic compartment (CCC) packed with chloroplasts and mitochondria and a peripheral layer of cytoplasm with chloroplasts (Voznesenskaya et al., 2002, 2005; Akhani et al., 2005). The CCC, which is surrounded by the vacuole, is connected to the peripheral cytoplasm by cytoplasmic channels. The leaves of *B. sinuspersici* differ anatomically by having mostly one to two layers of chlorenchyma cells, in comparison with two to three layers in *B. cycloptera*. Furthermore, *B. sinuspersici* is distinguished from *B. cycloptera* by having longer cotyledon

[1] This work was supported by the National Science Foundation (grant no. IBN–0641232).

* Corresponding author; e-mail edwardsg@wsu.edu.

The author responsible for distribution of materials integral to the findings presented in this article in accordance with the policy described in the Instructions for Authors (www.plantphysiol.org) is: Gerald E. Edwards (edwardsg@wsu.edu).

[OA] Open Access articles can be viewed online without a subscription.

www.plantphysiol.org/cgi/doi/10.1104/pp.108.124008

leaves and larger seeds, flowers, and chromosomes, together with a set of differences in micromorphological features (Akhani et al., 2005).

From studies on *Bienertia* species, the following model has been developed for C_4 photosynthesis. Atmospheric CO_2, upon entry into chlorenchyma cells, is incorporated into the C_4 acid oxaloacetate by PEPC in the peripheral cytoplasm. The C_4 acids malate and Asp, which are formed from the oxaloacetate, diffuse to the CCC through cytoplasmic channels, where malate is decarboxylated by NAD-malic enzyme (NAD-ME) in the mitochondria, which are specifically located in this compartment. Rubisco, located in chloroplasts in the CCC, fixes the released CO_2. The three-carbon product formed from C_4 acid decarboxylation (pyruvate or Ala) then diffuses to the peripheral chloroplasts, where pyruvate,Pi dikinase (PPDK) regenerates phospho*enol*-pyruvate from pyruvate for the PEPC reaction, which completes the C_4 cycle (Voznesenskaya et al., 2002; Edwards et al., 2004).

In studies on C_4 species with Kranz anatomy, much effort has been made to elucidate the mechanisms underlying cell differentiation and the selective synthesis of certain photosynthetic enzymes in mesophyll or bundle sheath cells. In the monocot maize (*Zea mays*), as a consequence of cell division patterns, a developmental gradient exists, with the oldest cells at the tip of the blade and the youngest at the base of the sheath. Both bundle sheath and mesophyll cells mature in concert with the vascular system and become photosynthetically competent in the same order as veins develop. Light is an essential component in determining leaf identity: studies with etiolated leaves indicate that Rubisco is present in both mesophyll and bundle sheath cell chloroplasts, while many of the C_4 enzymes are not expressed. After illumination, Rubisco expression becomes repressed in mesophyll cells and enhanced in bundle sheath cells, while C_4 enzymes accumulate. It is proposed that maize exhibits a C_3-type pattern of photosynthetic gene expression by default in the dark (Rubisco in all photosynthetic cells) and that C_4 specialization is achieved through the interpretation of light-induced signals from the leaf vasculature (Sheen and Bogorad, 1987; Langdale et al., 1988; Langdale and Nelson, 1991).

In contrast to maize, the initiation of specific localization of Rubisco in bundle sheath cells of *Amaranthus hypochondriacus* (dicot) can occur in cotyledons independent of light, as conversion from a C_3 default to a C_4 distribution pattern occurs in cotyledons of both dark- and light-grown seedlings. In young leaves of amaranth, mRNAs for Rubisco appear in both cell types, with light-dependent control of Rubisco expression in bundle sheath cells at the translational level. The expression of NAD-ME requires illumination, while PPDK and PEPC expression in mesophyll cells is independent of light. In leaves and cotyledons of this species, the early developmental process can influence the establishment of cell type-specific expression (Wang et al., 1992, 1993; Long and Berry, 1996). In both maize and amaranth, the establishment of mesophyll and bundle sheath cell-specific gene expression are separate events that occur during different stages of leaf development. Individual C_4 genes are independently regulated during cell type differentiation, and posttranscriptional regulation determines cell-specific patterns of expression very early in leaf development (Sheen, 1999; Patel et al., 2004; Patel and Berry, 2008).

The regulation, timing, and pattern of expression of photosynthetic genes for carbon assimilation in the single-cell C_4 system are addressed in this study. During development of the single-cell C_4 system in leaves of *B. sinuspersici* plants growing under moderate light (ML; 400 μmol quanta m^{-2} s^{-1} photosynthetic photon flux density [PPFD]), photosynthetic gene expression at the transcript and peptide levels was evaluated in relation to changes in leaf anatomy and the structure of chlorenchyma cells. In addition, the stability of transcripts, proteins, and the structure of C_4-type chlorenchyma cells following transfer to prolonged low light (LL; 20 PPFD) and prolonged darkness (D) treatments were studied.

RESULTS

Samples from leaves 0.1 to 0.3 cm (young stage), 0.5 to 0.6 cm (intermediate stage), and greater than 2 cm (mature stage) long were collected and analyzed. The young and intermediate leaves were divided into two parts, one containing the tip and the other containing the base of the leaf. The samples analyzed were designated as follows: young base (YB), young tip (YT), intermediate base (IB), intermediate tip (IT), and mature (M) leaf. Cross sections for analysis by microscopy were taken from the middle of each sample.

General Anatomy and Development during Growth under ML (400 PPFD)

Figure 1 shows the anatomy of leaves and the structure of chlorenchyma of the five samples in cross sections using light microscopy (left and middle panels) and the corresponding starch content (right panels). The YB contains from one to two layers of cells that will give rise to mature chlorenchyma and that are circumferentially distributed around the entire leaf just under the layer of large epidermal cells (Fig. 1, A and B). Beneath the chlorenchyma cells, there is a layer of water storage cells. All internal cells are rather tightly packed at this stage of development. The nuclei are distinct in various cell types, and at this stage in chlorenchyma cells they are in a central position where they occupy a large part of the cell volume, with no evidence of the development of a CCC. Some scattered starch grains appear within chlorenchyma cells (Fig. 1C). The anatomy of the YT is quite similar to that of the base, but with some differences: the epidermal cells are more uniform in size and shape (Fig. 1, D and

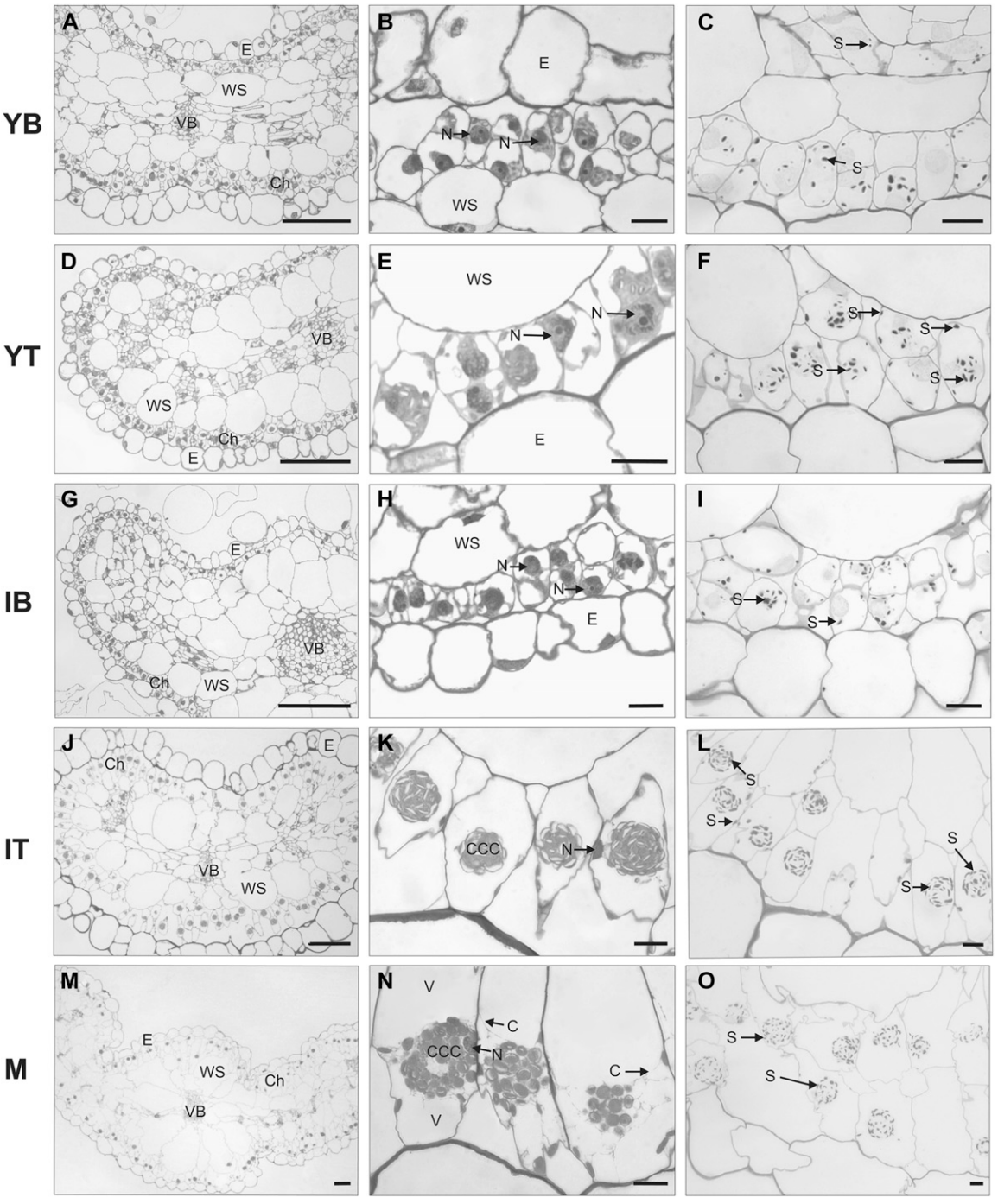

Figure 1. Light micrographs showing cross sections of leaf anatomy and chlorenchyma structure of *B. sinuspersici* plants grown under ML (400 μmol quanta m^{-2} s^{-1}) conditions. Young leaves (0.1–0.3 cm) were divided into two parts, YB (A–C) and YT (D–F). Intermediate-sized leaves (0.5–0.6 cm) were divided into two parts, IB (G–I) and IT (J–L). Cross sections of M leaves (>2 cm) are shown in M to O. PAS staining for polysaccharides showing starch grains is shown in C, F, I, L, and O. Cross sections were taken from the middle of each sample. C, Cytoplasmic channels; Ch, chlorenchyma cells; E, epidermis; N, nucleus; S, starch; V, vacuole; VB, vascular bundles; WS, water storage tissue. Bars = 100 μm (left panels) and 10 μm (middle and right panels).

E), the nuclei of chlorenchyma cells are not as large, and the starch content is increased with respect to that of the base (Fig. 1F).

Samples from intermediate leaves are shown in Figure 1, G to L. At this stage of development, the differences between the base and the tip are more pronounced, with evidence of a gradient of development from the base to the tip. While chlorenchyma cells in the base are still tightly packed and have a prominent central nuclei (Fig. 1, G and H) and some

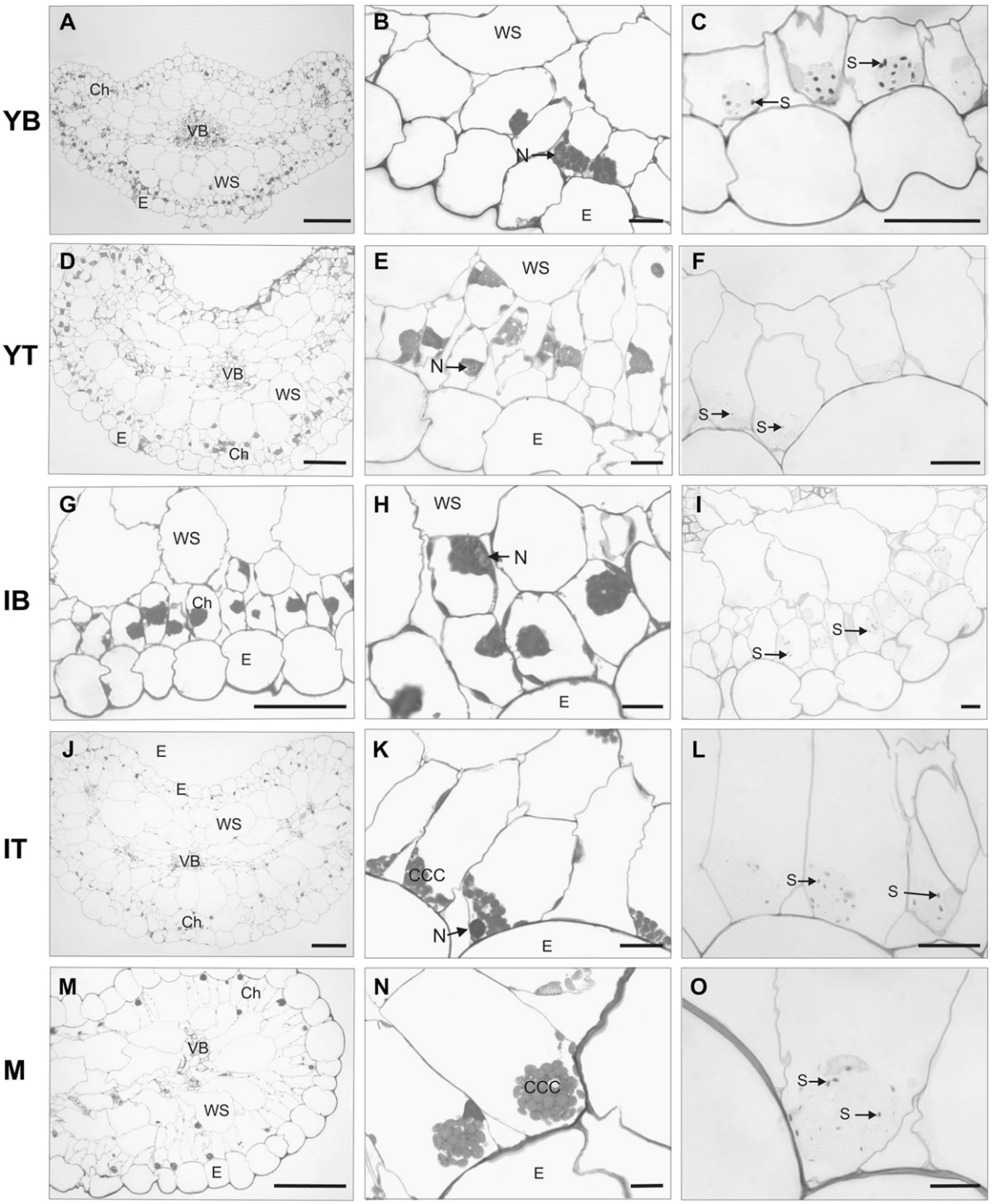

Figure 2. Light micrographs showing cross sections of leaf anatomy and chlorenchyma structure of *B. sinuspersici* plants grown under ML conditions (400 μmol quanta m^{-2} s^{-1}) and then transferred to LL (20 μmol quanta m^{-2} s^{-1}) for 1 month. Young leaves (0.1–0.3 cm) were divided into two parts, YB (A–C) and YT (D–F). Intermediate-sized leaves (0.5–0.6 cm) were divided into two parts, IB (G–I) and IT (J–L). Cross sections of M leaves (>2 cm) are shown in M to O. PAS staining for polysaccharides showing starch grains is shown in C, F, I, L, and O. Cross sections were taken from the middle of each sample. Abbreviations are as in Figure 1. Bars = 100 μm (left panels) and 10 μm (middle and right panels).

starch content (Fig. 1I), chlorenchyma cells in the tip are more differentiated and have extensively developed intercellular air spaces. These cells are bigger, ellipsoid, and have formed a CCC filled with chloroplasts, with the nucleus located near the periphery of the cell. Some chloroplasts are also observed in the peripheral cytoplasm. The size of water storage cells is also increased at this stage (Fig. 1, J and K). Starch has

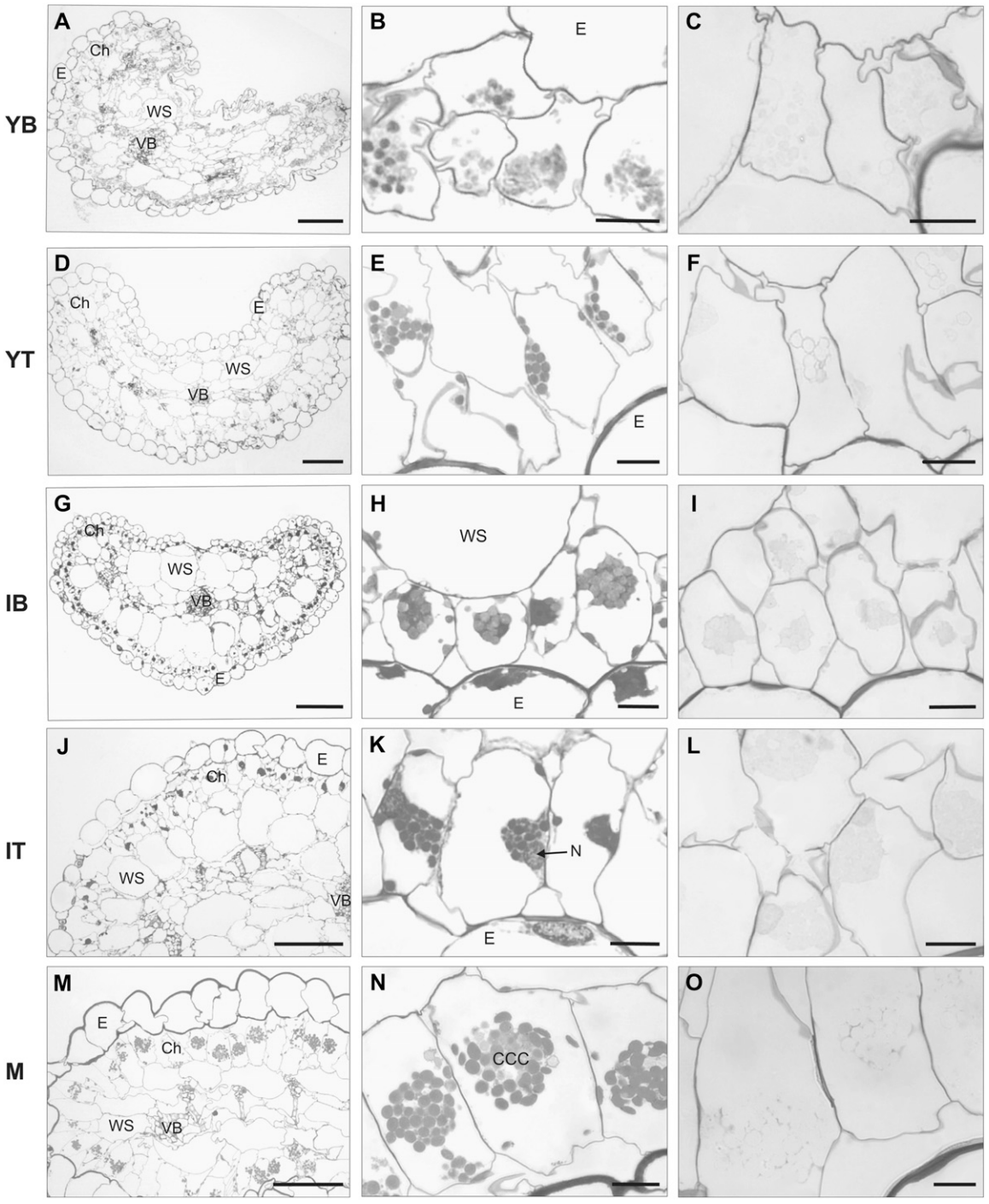

Figure 3. Light micrographs showing cross sections of leaf anatomy and chlorenchyma structure of *B. sinuspersici* following prolonged exposure of part of the plant to D for 1 month. Young leaves (0.1–0.3 cm) were divided into two parts, YB (A–C) and YT (D–F). Intermediate-sized leaves (0.5–0.6 cm) were divided into two parts, IB (G–I) and IT (J–L). Cross sections of M leaves (>2 cm) are shown in M to O. PAS staining for polysaccharides showing starch grains is shown in C, F, I, L, and O. Cross sections were taken from the middle of each sample. Abbreviations are as in Figure 1. Bars = 100 μm (left panels) and 10 μm (middle and right panels).

accumulated mainly in the chloroplasts of the CCC, but a small amount of starch is also observed in the peripheral chloroplasts (Fig. 1L).

In M leaves, there are one to two layers of chlorenchyma cells that appear quite similar to those in IT samples (Fig. 1, M and N). The CCC is well formed,

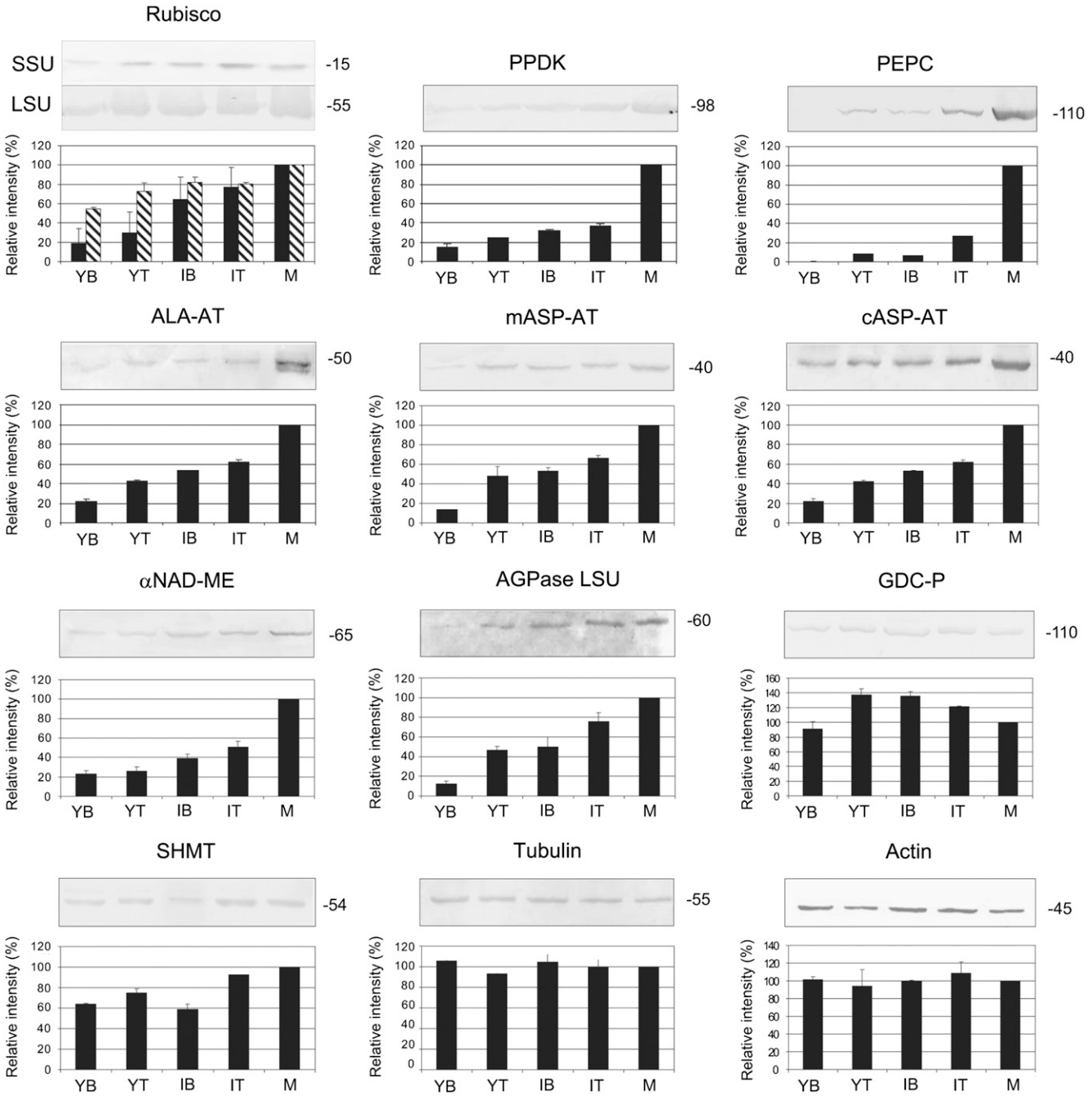

Figure 4. Western-blot analysis of proteins involved in photosynthesis of *B. sinuspersici* that were isolated at different stages of leaf development from plants grown under ML (400 μmol quanta m^{-2} s^{-1}). Western blots were obtained using antibodies against PPDK, PEPC, αNAD-ME, Rubisco SSU (solid), Rubisco LSU (hatched), ALA-AT, mASP-AT, cASP-AT, AGPase LSU, GDC-P, SHMT, tubulin, and actin. Twenty micrograms of total soluble protein was added per lane, except for Rubisco LSU, for which 5 μg was loaded per lane. Molecular masses of the immunoreactive bands are shown on the right and expressed in kilodaltons. The quantification of the immunoreactive bands is expressed as a percentage of the amount in M leaves and shown below each western blot (n = 2 or 3). SD values are shown.

and starch is restricted to this compartment (Fig. 1O). Nuclei, which are positioned adjacent to the CCC, are generally close to the radial cell wall. Cytoplasmic channels connecting the CCC and the periphery of the cells are well established at this stage of development (Fig. 1N). The prominent vacuole extends from the CCC to the distal and proximal ends of the cell.

Throughout development, the vascular bundles are arranged in a lateral longitudinal plane with a main, large central vascular bundle (Fig. 1A).

General Anatomy after Transfer and Maintenance of Plants under LL (20 PPFD)

We tested the effects of the exposure of plants to very LL intensity on leaf anatomy and the structure of chlorenchyma cells of *B. sinuspersici*. Plants were transferred from growth under ML (400 PPFD) to a LL chamber (20 PPFD), and leaf tissue was analyzed after 1 month (Fig. 2). Different stages of leaf development were examined, analogous to those under ML growth conditions (Fig. 1). Samples of young and intermediate leaves that developed under LL, and samples of leaves that were mature prior to prolonged exposure to LL, were analyzed (due to limited growth under LL, there was no development of M leaves). Exposure of plants to the LL regime did not cause a significant change in leaf general anatomy, as there was conservation of different layers of tissue with respect to cell size and shape (Fig. 2). However, exposure of plants to LL had a large influence on the position of the CCC in the IT (Fig. 2, J and K) as well as in the M leaf (Fig. 2, M and N). In both cases, although there is a separate compartment containing tightly packed chloroplasts, it is not located in the center of the cell but rather at the periphery, typically at the distal end near the epidermis, and the nucleus remains close to the cytoplasmic ball. Since the IT leaf sections formed during LL treatment, it indicates that the cytoplasmic ball develops and is positioned to the periphery of the cell under LL conditions. However, in M leaves that developed prior to LL treatment, the CCC shifted from the center to the periphery of the cells following prolonged exposure to LL (see above). As

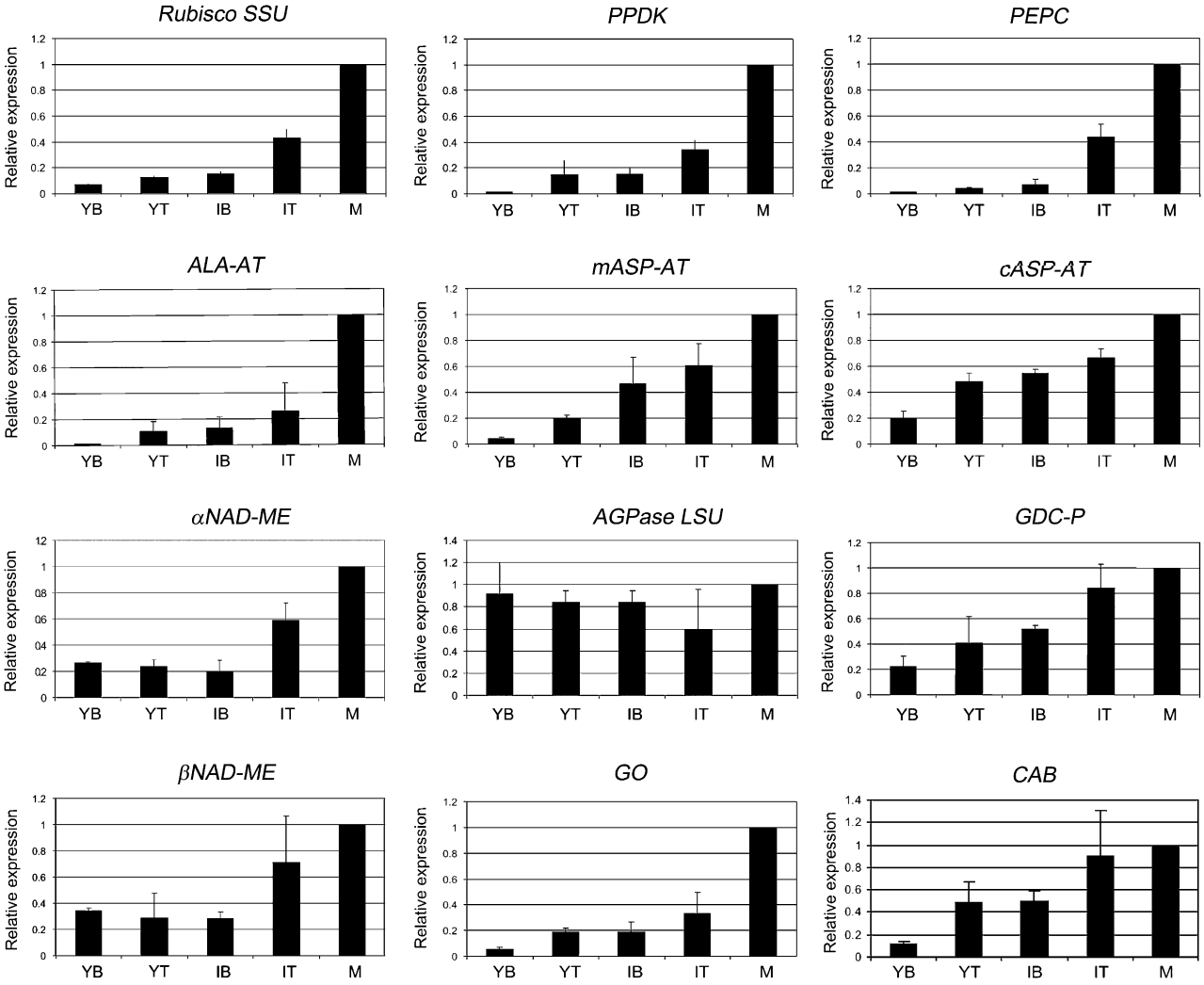

Figure 5. Expression analysis of transcripts of enzymes involved in photosynthesis in leaves of *B. sinuspersici* during development under ML (400 μmol quanta m^{-2} s^{-1}), as determined by QRT-PCR. Analyses were made with RNA isolated from leaves at different stages of development: YB, YT, IB, IT, and M leaves. The means of the results obtained, using three independent RNAs as a template, are shown. Each reaction was normalized using the C_t values corresponding to *B. sinuspersici* elongation factor 1 gene. The *y* axis shows the fold difference in a particular transcript level relative to its amount found in M leaves. SD values are shown.

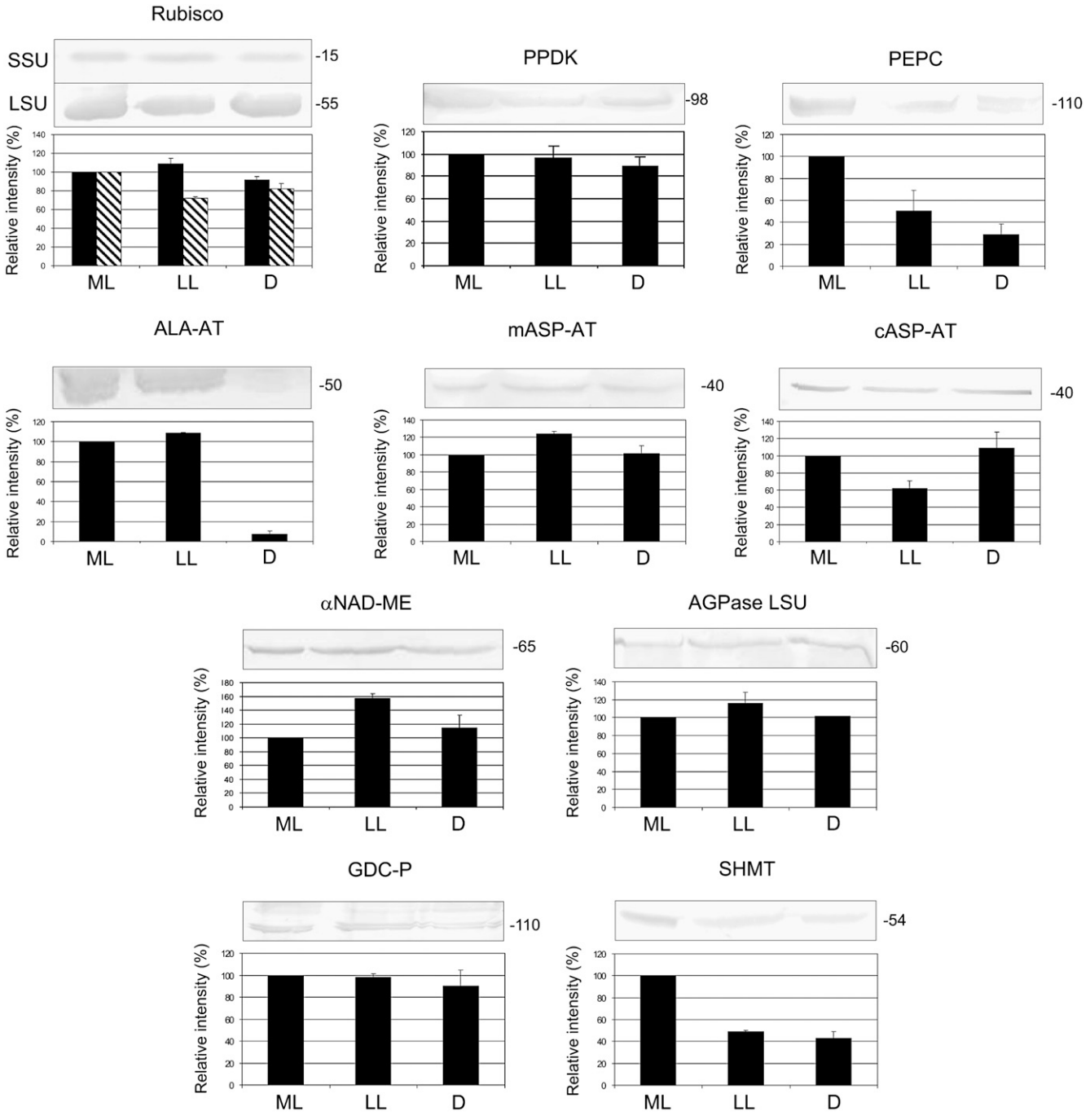

Figure 6. Western-blot analysis of proteins involved in photosynthesis of *B. sinuspersici* that were isolated from M leaves exposed to different illumination conditions. Western blots were obtained using antibodies against PPDK, PEPC, αNAD-ME, Rubisco SSU (solid), Rubisco LSU (hatched), ALA-AT, mASP-AT, cASP-AT, AGPase LSU, GDC-P, and SHMT. Twenty micrograms of total soluble protein was added per lane, except for Rubisco LSU, for which 5 μg was loaded per lane. ML, M leaves from plants grown under ML intensities (400 μmol quanta m^{-2} s^{-1}); LL, M leaves developed under ML conditions followed by exposure of plants to LL conditions (20 μmol quanta m^{-2} s^{-1}); D, branches of plants growing under ML were enclosed in continuous D. Molecular masses of the immunoreactive bands are shown on the right and expressed in kilodaltons. The quantification of the immunoreactive bands is expressed as a percentage of the amount in M leaves grown under ML and shown below each western blot ($n = 2$ or 3). SD values are shown.

expected, due to reduced energy supply for photosynthesis, the starch content was low at all stages of leaf development (Fig. 2, C, F, I, L, and O), with the exception of YB leaf sections, in which some starch appears similar to that in YB leaf sections in plants grown in ML (Fig. 1C).

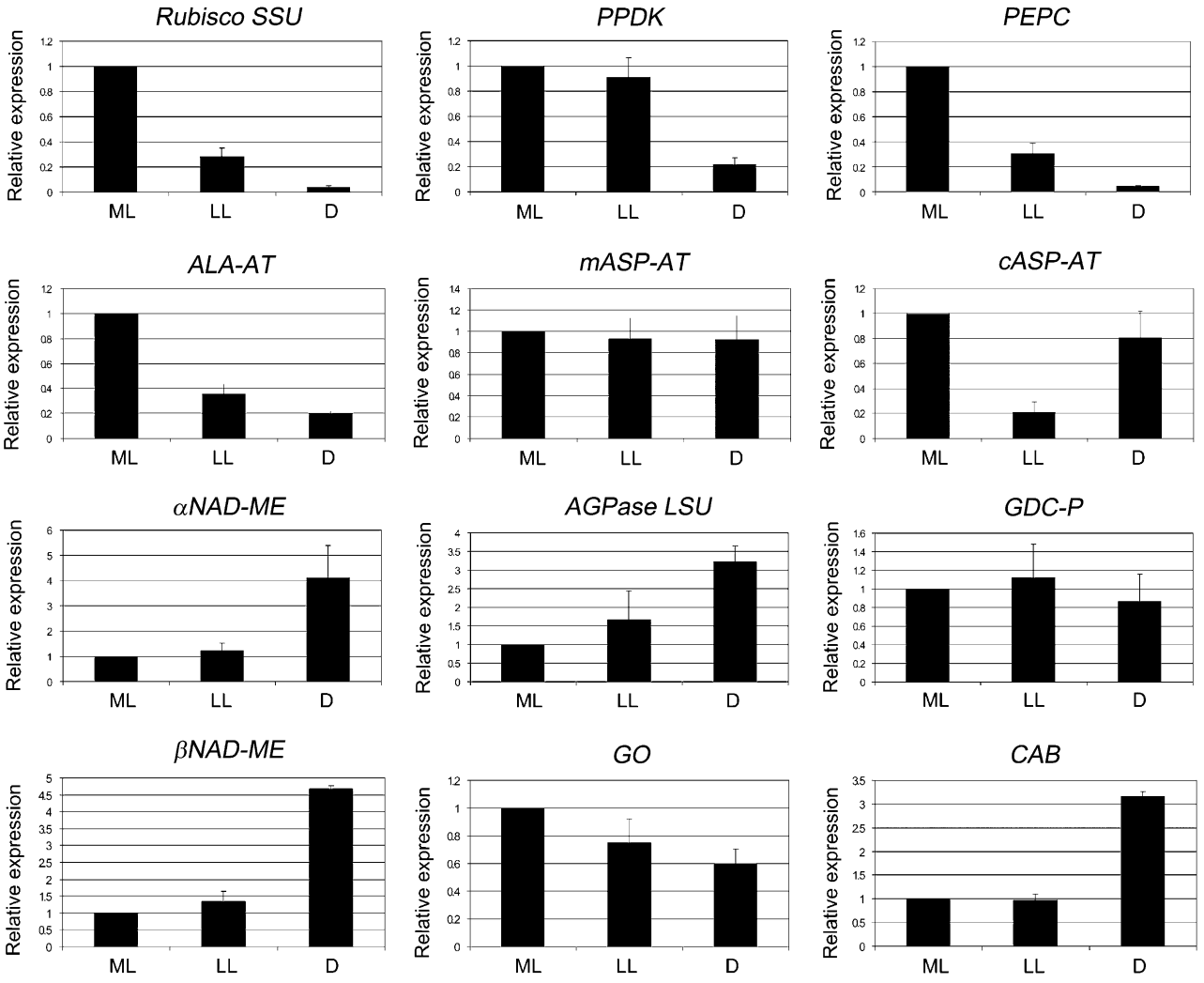

Figure 7. Effect of illumination conditions during growth on transcript expression of photosynthetic genes in M leaves of *B. sinuspersici*, as determined by QRT-PCR. ML, M leaves from plants grown under ML intensities (400 μmol quanta m^{-2} s^{-1}); LL, M leaves developed under ML conditions followed by exposure of plants to LL conditions (20 μmol quanta m^{-2} s^{-1}); D, branches of plants growing under ML were enclosed in continuous D. The means of the results obtained, using three independent RNAs as a template, are shown. Each reaction was normalized using the C_t values corresponding to *B. sinuspersici* elongation factor 1 gene. The *y* axis shows the fold difference in a particular transcript level relative to its amount found in M leaves grown under ML intensities (400 μmol quanta m^{-2} s^{-1}). SD values are shown.

General Anatomy of Vegetative Tissue Exposed to Continuous D

When branches of plants growing under ML were enclosed in continuous D for 30 d, cross sections of leaves at various stages of development (Fig. 3) showed leaf anatomy similar to that of light-exposed leaves (Fig. 1). In the younger and intermediate leaves that developed in D (Fig. 3), there is clear initiation of development of the two cytoplasmic domains, with the chloroplasts aggregating adjacent to the nucleus to form the CCC and isolated chloroplasts in the periphery. In the M leaves that developed prior to enclosure in D, the chlorenchyma cells retain the CCC (Fig. 3, K and N). However, there was an obvious dispersal and loosing of the CCC compared to M leaves grown under ML conditions (Fig. 1). In branches maintained in D for 1 month, no starch was visualized in any chloroplasts from leaves examined at different stages of development (Fig. 3C, F, I, L, and O).

Levels of Transcripts and Peptides Involved in C_4 Photosynthesis

The levels of a number of proteins associated with the photosynthetic apparatus of C_4 photosynthesis were semiquantified by western-blot analysis in leaves at different developmental stages grown in growth chambers (Fig. 4) as well as in M leaves treated under prolonged LL or D conditions (Fig. 6). In addition, the levels of transcripts encoding a majority of these pro-

teins were also quantified by quantitative real-time reverse transcription-PCR (QRT-PCR; Figs. 5 and 7).

Analysis during Leaf Development under ML Growth Conditions

With respect to western-blot analysis, anti-tubulin and anti-actin antibodies were used as indicators that the same level of protein was loaded in each lane. Actin and microtubules appear very early in young chlorenchyma tissue (J. Park, M. Knoblauch, T. Okita, and G. Edwards, unpublished data); with cell expansion and development of organelles, the filaments and cables are arranged in an organized network in mature C_4 chlorenchyma (Chuong et al., 2006); there appears to be a parallel increase in total protein content and the cytoskeleton during development of the leaf tissue. Quantification of the intensity of the bands was conducted by image analysis software, and the mean value of the immunoreactive bands in M leaves was arbitrarily set as 100% (Fig. 4). Transcript expression levels obtained by QRT-PCR were normalized using elongation factor 1 as a reference gene, and results for YB, YT, IB, and IT samples are expressed relative to the values obtained for M leaves (Fig. 5). The levels of Rubisco small subunit (SSU) polypeptide were low, with YB having only approximately 20% of that of M leaves and YT only 30% of that of M leaves. The transcript levels for *SSU* were also rather low in YB tissue and increased during development, particularly in IT and M leaves. There was substantial Rubisco large subunit (LSU) polypeptide in the youngest tissue, with YB leaf sections having approximately 50% of that in M leaves, and the level gradually increased during leaf development (Fig. 4).

As Rubisco LSU is encoded by the chloroplastic genome and therefore lacks the typical eukaryotic poly(A) tail, which is (in turn) required for reverse transcription by the method applied in this study [oligo(dT) primer method], transcripts for Rubisco LSU were not determined.

Peptides and transcripts for six C_4 cycle enzymes were studied during leaf development (PPDK, PEPC, Ala aminotransferase [ALA-AT], mitochondrial and cytosolic Asp aminotransferase [mASP-AT and cASP-AT], and αNAD-ME). With respect to enzymes involved in the C_4 cycle, both protein and transcript levels were very low (from 0% to approximately 20% of M leaves) during early stages of development and increased to the highest level in M leaves. In YB leaves, PEPC protein was not visualized by western blot (Fig. 4) and its transcript was barely detected (Fig. 5). Very low levels of proteins and transcripts were observed in YT and IB samples, with some increase in IT samples and a large increase in M leaves (Figs. 4 and 5). PPDK, ALA-AT, cASP-AT, and mASP-AT showed a large increase in protein and transcript levels during development (Figs. 4 and 5). The αNAD-ME peptide and transcripts encoding for both α- and β-subunits showed a similar pattern of increase (approximately 4-fold) from YB to M leaves (Figs. 4 and 5).

With respect to ADP-Glc-pyrophosphorylase (AGPase), which is required for starch biosynthesis, there was a large increase in the LSU peptide during development, whereas there were high transcript levels of *AGPase LSU* at all stages (Figs. 4 and 5).

Some of the key proteins of photorespiration were analyzed during leaf development. There were high levels of the P subunit protein of Gly decarboxylase (GDC-P) and of Ser hydroxymethyltransferase (SHMT) throughout development (Fig. 4). However, transcript levels for *GDC-P* and *GLYCOLATE OXIDASE* (*GO*) increased during development (Fig. 5). When *CHLOROPHYLL A/B-BINDING PROTEIN* (*CAB*) transcript expression was analyzed, it was found in lower levels in YB samples, in intermediate amounts in YT and IB samples, and at maximum content in IT and M leaf samples (Fig. 5).

Analyses of M Leaves following Prolonged Treatment under LL or D

The effect of prolonged exposure of plant tissue to LL and D on levels of proteins and transcripts associated with C_4 photosynthesis was investigated (Figs. 6 and 7). Again, elongation factor 1 was used as a reference gene for QRT-PCR, and results are expressed in relation to the values obtained under ML growth conditions. Analyses were made on leaves that had reached maturity under ML, prior to exposure for 1 month to LL or D conditions. The results show that the levels of many of the peptides analyzed were retained, or largely retained, during LL and D treatments for 1 month (Fig. 6), including Rubisco SSU (equivalent to plants under ML

Table I. *Carbon isotope discrimination and water, total soluble protein, and chlorophyll contents in B. sinuspersici M leaves grown under different illumination conditions*

DM, Dry mass; FM, fresh mass. M leaves were collected from plants grown under ML (400 PPFD) conditions, from plants grown under ML light and then exposed to LL (20 PPFD) for 1 month (LL treatment), and from branches of plants exposed to continuous D for 1 month while growing under ML (D treatment). Values represent means of at least three independent determinations (SD values are shown).

Sample	$\delta^{13}C$	Water	Total Chlorophyll ($a + b$)		Total Soluble Protein	
	‰	% FM	$\mu g\ mg^{-1}$ DM	$\mu g\ mg^{-1}$ FM	$\mu g\ mg^{-1}$ DM	$\mu g\ mg^{-1}$ FM
ML	−17.4 ± 0.7	89.6	2.13 ± 0.57	0.22 ± 0.06	26.0 ± 0.28	2.71 ± 0.03
LL	−20.0 ± 0.5	95.1	1.03 ± 0.37	0.05 ± 0.02	13.0 ± 0.12	0.64 ± 0.01
D	−20.3 ± 0.1	87.4	4.04 ± 0.10	0.51 ± 0.07	20.9 ± 0.24	2.62 ± 0.03

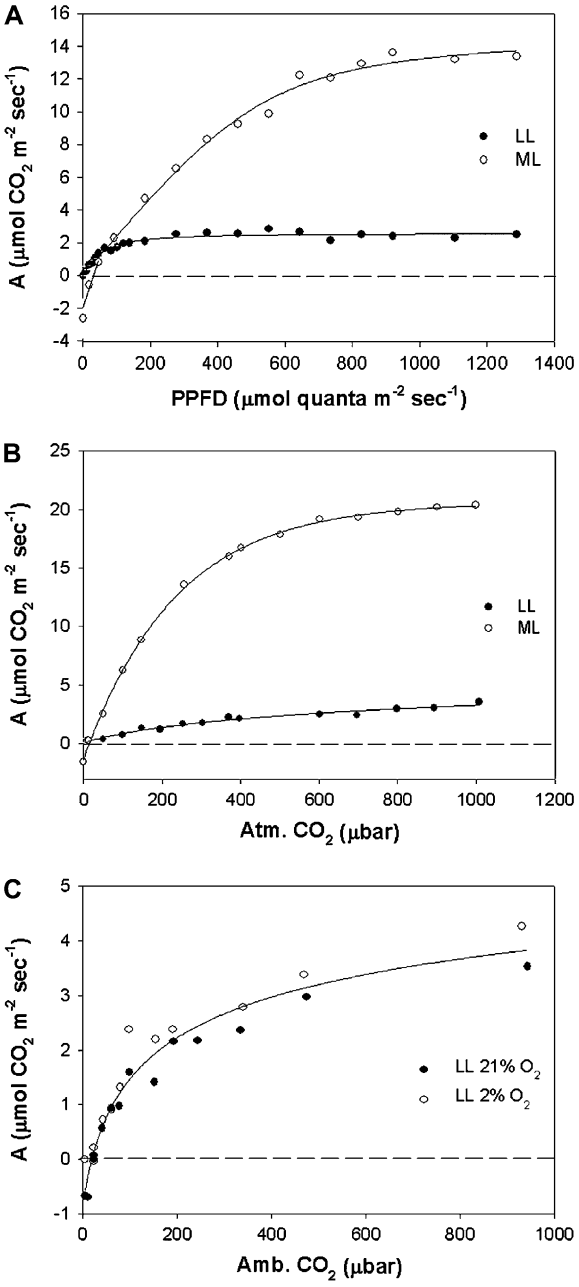

Figure 8. A, Light response curves of *B. sinuspersici* at 340 μbar CO_2. B, The response of photosynthesis to varying levels of atmospheric CO_2 at 1,000 μmol quanta m^{-2} s^{-1}. C, Response of photosynthesis of LL-treated plants to varying levels of CO_2 under 2% versus 21% O_2. White and black symbols denote *B. sinuspersici* grown in ML (400 μmol quanta m^{-2} s^{-1}) and LL (20 μmol quanta m^{-2} s^{-1}) intensities, respectively. For A and B, the results represent the average of three replicates on three separate branches. For C, the results are from individual measurements at 2% versus 21% O_2 (at a given C_i from two experiments on separate branches).

growth), LSU (20%–30% drop), PPDK, cASP-AT and mASP-AT, αNAD-ME, AGPase LSU, and GDC-P. However, there was a large decline of PEPC and SHMT proteins in both LL and D treatments and a dramatic loss of ALA-AT in D treatment. Transfer of plants to LL conditions for 1 month caused a profound drop in transcript levels for *Rubisco SSU* and three C_4 cycle enzymes, *PEPC*, *ALA-AT*, and *cASP-AT*. Also, under D treatment, *Rubisco SSU* and *PEPC* transcripts were severely reduced (to a few percentage points of regular light conditions), while *PPDK* and *ALA-AT* decreased to approximately 20% of ML growth (Fig. 7). There were notable increases in transcripts in D-treated leaves for *αNAD-ME* and *βNAD-ME* and for *CAB* (approximately 3- to 4-fold increase). Under LL and D treatments, *mASP-AT*, *AGPase LSU*, and two photorespiratory enzymes, *GO* and *GDC-P*, had the highest levels of transcripts (60% or more relative to ML growth conditions).

Leaf Composition: Chlorophyll, Protein, Water Content, and Carbon Isotope Values

Chlorophyll, soluble protein, water content, and carbon isotope values (δ ^{13}C) were measured to determine the effects of LL and D treatments on leaf composition (Table I). The δ ^{13}C value for M leaves under ML growth conditions was $-17.4‰$, whereas values for M leaves exposed to 1 month of LL or D were more negative, approximately $-20‰$. The M leaves on plants exposed to 1 month of LL were noticeably larger and pale green compared with those on plants grown under ML. The LL leaves had a higher water content expressed as percentage of fresh mass and much lower chlorophyll content and total soluble protein content on a dry or fresh weight basis than ML-grown plants (Table I). The D-treated tissue had similar water content (percentage of fresh mass) and similar levels of soluble protein as ML-grown leaves. However, the total chlorophyll ($a + b$), both on a fresh and a dry mass basis, was twice as high in M leaves under the D treatment as in leaves maintained under ML (Table I).

The δ ^{13}C values were also determined on leaf sections during development under ML. For YB, YT, IB, and IT, the values were very similar, $-19.8‰$, $-20.1‰$, $-20.8‰$, and $-20.3‰$, respectively, compared with $-17.4‰$ for ML.

Response of Photosynthesis to Varying Light and CO_2 under ML Growth versus LL Treatment

The rate of photosynthetic CO_2 fixation in *B. sinuspersici* was measured at varying light intensities and at 340 μbar CO_2 on plants grown under ML conditions versus plants exposed to prolonged LL conditions. Figure 8A shows that plants grown under ML conditions have a much higher capacity for photosynthesis, a higher light compensation point (31 PPFD), and higher rates of dark respiration (approximately 2 μmol m^{-2} s^{-1}) than LL-treated plants. Photosynthesis in LL-treated plants was saturated at approximately 200 PPFD, while in plants in ML growth conditions, approximately 1,000 PPFD was required for light saturation. The photosynthetic response to varying levels of CO_2 under 1,000 PPFD was compared in plants from ML growth conditions versus LL treatment, again

showing that plants grown under higher PPFD have much higher CO_2-saturated rates of photosynthesis (Fig. 8B). With plants under ML growth and LL treatment, the rate of photosynthesis at current ambient levels of CO_2 (approximately 370 μbar) was about 75% of the CO_2-saturated rate at 1,000 μbar CO_2 (Fig. 8, B and C). The values for the CO_2 compensation points were low for both ML growth and LL conditions (approximately 10 μbar CO_2; Fig. 8B). The response of photosynthesis of LL-treated plants to varying levels of CO_2 under 2% versus 21% O_2 is shown in Figure 8C. The results show that the CO_2 response curve is similar under the two levels of O_2, with no apparent affect of O_2 on rates of photosynthesis under limiting CO_2.

DISCUSSION

We studied the pattern of leaf development in *B. sinuspersici* together with the expression of a number of proteins associated with C_4 photosynthesis, including enzymes of the C_4 cycle. The influence of the exposure of plants to extreme LL on the function of C_4 photosynthesis and of enclosure of branches in D on photosynthetic transcripts and protein level, and on the structure of chlorenchyma cells, was evaluated.

Development of Single-Cell C_4 Photosynthesis during ML Growth Conditions

Five developmental stages were analyzed in *B. sinuspersici*: the base and tip of very young leaves (YB and YT), the base and tip of intermediate leaves (IB and IT), and M leaves during ML growth. Leaves of *B. sinuspersici* (this work) and *B. cycloptera* (Voznesenskaya et al., 2005) have acropetal leaf development. There was a gradient of development and cellular differentiation from the base to the tip of the leaves, with the tip being at a more advanced stage than the base. This is very evident in intermediate leaves, where the anatomy of the tip is quite similar to that of the M leaf, while the base is still quite undifferentiated (Fig. 1).

YB Leaf Sections

In chlorenchyma cells in the base of the young leaf, the nucleus is a dominant organelle in the cytoplasm, along with the surrounding chloroplasts, which occupy much of the cytoplasmic space (also, in *B. cycloptera*, the very youngest newly emerged leaves [less than 1 mm in length] are cytoplasmically dense and have little vacuole development [Voznesenskaya et al., 2005]). In *B. sinuspersici*, starch grains are present at this earliest stage in chlorenchyma cells; however, they have a scattered arrangement (Fig. 1C). There is no evidence of polarization toward the development of two cytoplasmic compartments.

In analysis of a number of photosynthetic proteins by western blot, there was substantial Rubisco LSU in YB leaf sections (55% of M leaves) compared with Rubisco SSU, with levels of approximately 20% of M leaves; the levels of both subunits increased progressively during development. The results suggest that in very young tissue, the LSU may be synthesized in excess prior to the production of equivalent SSU for assembly of the holoenzyme. In the YB, the transcript levels for the *Rubisco SSU* were also low (approximately 10% of M leaves) and increased during development. AGPase LSU was low in YB tissue and increased progressively during development, while levels of *AGPase LSU* transcripts were relatively high throughout leaf development (Figs. 4 and 5), which suggests that there may be posttranscriptional control of the synthesis of the LSU. This posttranscriptional control is most likely caused by lower expression of the counterpart *AGPase SSU* gene, which is required for the stability of the LSU (Wang et al., 1998).

Peptides and transcripts were analyzed in YB tissue for six enzymes known to function in the C_4 cycle in NAD-ME-type C_4 species (PPDK, PEPC, ALA-AT, mASP-AT, cASP-AT, and αNAD-ME; Figs. 4 and 5). In contrast to Rubisco LSU and SSU, PEPC protein was practically undetectable in YB tissue. PEPC protein and transcripts remained very low during development until the IT stage. There was a similar pattern with the five other C_4 enzymes, in which transcripts and peptides were rather low in YB tissue (from barely detectable levels to approximately 20% of that of M leaves) and thereafter increased during development. There were substantial levels of two photorespiratory enzymes, GDC-P and SHMT, in YB leaf sections, similar to that at later stages of development. The levels of transcripts of photorespiratory proteins, *GO* and *GDC-P*, were lower in YB, increasing during development.

The early appearance of Rubisco LSU, GDC-P, and SHMT in YB leaves and the later rise in C_4 cycle enzymes suggest that chloroplasts in YB tissue may be functioning in a C_3 default mode with metabolism in the C_3 cycle and photorespiratory pathway. Previous studies on immunolocalization in *B. cycloptera* showed that all chloroplasts in young chlorenchyma cells contain Rubisco LSU and that the biomass of young tissue has more negative δ ^{13}C values than M leaves, which is consistent with young leaves performing C_3 photosynthesis (Voznesenskaya et al., 2005).

YT and IB Leaf Sections

In YT and IB leaf sections, there is evidence for some chloroplasts aggregating near the nucleus, which suggests an early stage of formation of the CCC (Fig. 1, E and H); also, staining for starch shows colocalization of starch grains in some chlorenchyma cells in YT and IB leaf sections (Fig. 1, F and I). In contrast to the relatively high levels of Rubisco LSU in these tissues (approximately 75% of that of M leaves), PEPC peptides and transcripts remain very low. Levels of peptides of the five other C_4 cycle enzymes in YT and IB are approximately 20% to 40% of those in M leaves, and transcript levels for these respective enzymes are approximately 10% to 40% of those of M leaves. In addition, in almost

every case analyzed, the levels of transcripts are similar in YT and IB samples. In YT and IB leaf tissue, the lack of full development of C_4 biochemistry and of the two cytoplasmic compartments would limit the function of C_4.

IT and M Leaves

In IT and M leaf tissue, the CCC and the peripheral cytoplasmic compartments with chloroplasts partitioned to each have clearly formed. However, only in M leaves are the cytoplasmic strands connecting the CCC with the periphery very apparent and appearing well developed (Fig. 1N). As with *B. cycloptera* (Voznesenskaya et al., 2005), cell expansion appears to be required to accommodate the large structure of the CCC within the cell. Although some elongation of chlorenchyma cells is observed in the YT leaves, this is more evident in the IT samples. The levels of peptides for Rubisco SSU and LSU, GDC-P, SHMT, and AGPase LSU in IT leaf sections range from approximately 80% to 100% of the levels in M leaves. However, the level of PEPC in IT tissue is approximately 25% of that of M leaves, and the levels of the five other C_4 cycle enzymes analyzed are approximately 40% to 60% of that of M leaves (Fig. 4).

Thus, this study shows that, during leaf development of *B. sinuspersici*, the expression of C_4 enzymes clearly lags behind that of Rubisco LSU, AGPase LSU, and photorespiratory enzymes. In this regard, a recent study in the C_4 plant maize compared transcript levels for a number of nuclear, chloroplast, and mitochondrial genes at the green tip of the leaf compared with the yellow base of the leaf (which was surrounded by several layers of more M leaves). The tip-base ratio of transcripts for the following nuclear genes encoding enzymes in carbon assimilation was reported (ratio in parentheses): *Rubisco SSU* (15), *PPDK* (61), and *PEPC1* (68; Cahoon et al., 2008). In this study with *B. sinuspersici*, the ratios of M leaves to YB were (ratio in parentheses): *Rubisco SSU* (14), *PPDK* (83), and *PEPC* (85), which shows a similar trend to that of maize. The increase in *B. sinuspersici* of *CAB* transcripts during development may be related to the establishment of the light-harvesting antennae. Cahoon et al. (2008) also reported an increase in transcript levels for several chlorophyll *a*/*b*-binding proteins during leaf development in maize.

In *B. sinuspersici*, starch appears at all stages of development, and it becomes more concentrated in the CCC in IT and M leaves (Fig. 1, C, F, I, L, and O), which corresponds to the large increase in the AGPase LSU during development. In IT leaf sections, starch is expressed in the CCC (Fig. 1L), but it also appears in the peripheral chloroplasts; only in M leaves is starch confined to the CCC (Fig. 1O). In previous studies, it has been shown among various C_4 species in family Chenopodiaceae that only Rubisco-containing chloroplasts tend to accumulate starch (Voznesenskaya et al., 1999, 2003, 2005). In leaves of both Kranz and single-cell C_4 species, starch accumulates in mature Rubisco-containing chloroplasts and not in chloroplasts specialized to support the synthesis of C_4 acids by generating the substrate for PEPC. In *B. sinuspersici*, starch staining is scattered in the YB leaf section prior to the formation of the CCC (Fig. 1C). In the YT and IB sections, there are areas in which starch is more concentrated (Fig. 1, F and I), suggestive of the initial formation of a pre-CCC along with some scattered staining of starch. In IT sections where the CCC has clearly formed, it has strong staining for starch, with starch also appearing in the peripheral chloroplasts (Fig. 1L). In M leaves, the starch is completely confined to the CCC. It is not until the M stage that starch is no longer observed in chloroplasts in the periphery (Fig. 1O). This is consistent with a previous study with *B. cycloptera*, in which starch accumulated in young chlorenchyma cells but only became fully associated with the CCC in M leaves; immunolocalization studies showed that Rubisco followed the same pattern (Voznesenskaya et al., 2005).

While the CCC appears in IT sections (Fig. 1K), the cytoplasmic channels interconnecting with the peripheral cytoplasm appear more developed in M leaves (Fig. 1N). These results show that there is not a quick transition but a progressive development, both structurally and biochemically, which allows M leaves to perform C_4 photosynthesis.

The $\delta\ ^{13}C$ value for M leaves in this study was $-17.4‰$, which is C_4 like and may reflect the accumulation of biomass in leaves during the course of the structural and biochemical changes required for the development of a fully functional C_4 system. *B. sinuspersici* specimens collected from natural habitats have C_4-type $\delta\ ^{13}C$ values, on average $-13.8‰$, with a maximum of $-15.3‰$ (Voznesenskaya et al., 2002; Akhani et al., 2005). Typical values for C_4 plants are approximately $-10‰$ to $-15‰$ versus $-24‰$ to $-30‰$ for C_3 plants (Akhani et al., 1997; Cerling, 1999). Young leaf tissue of *B. sinuspersici* (YB, YT, and IB) obviously have not developed chlorenchyma tissue to perform C_4; their intermediate $\delta\ ^{13}C$ values (approximately $-20‰$) apparently reflect the partial dependence of young tissue on importing assimilates from M leaves, which would carry a C_4-type carbon isotope signature. The IT tissue has developed features of C_4 chlorenchyma, although they are less complete than those of ML tissue; the intermediate $\delta\ ^{13}C$ of IT leaf sections suggests less efficient function of C_4 than in ML. Online measurements of isotope fractionation during the photosynthesis of leaves at different stages of development will be required to directly relate the capacity and mode of photosynthesis to structural and biochemical features.

Effects of LL Treatment

Plants of *B. sinuspersici* grown under ML conditions were transferred to a LL chamber for 1 month, after which leaf anatomy and levels of peptides and transcripts of a number of photosynthetic proteins were

analyzed. There was little new growth during this period (only some young and intermediate leaves) due to the LL (20 PPFD).

In YT, IB, and IT leaf sections (Fig. 2, D, E, G, H, J, and K), there was evidence that new leaves formed under these very LL conditions had partial development of a cytoplasmic ball of chloroplasts adjacent to the nucleus. A striking difference compared with ML-grown plants was the location of this grouping of chloroplasts toward the periphery of the cells, compared with the typical centralized location under ML growth. YB leaf sections accumulated starch (Fig. 2C), perhaps from importing sugars from M leaves, whereas the starch levels were rather low at later developmental stages (Fig. 2, F, I, L, and O).

In M leaves that developed during growth under ML conditions, the CCC shifted to the periphery of the cell during the LL treatment, usually toward the distal end (i.e. shifting toward the limiting light source; Fig. 2, M and N). Cytoskeletal components, actin filaments and microtubules, have been found to participate in chloroplast movement (Kandasamy and Meagher, 1999; Sheahan et al., 2004). In response to the amount and quality of light, these organelles change their position and orientation (Williamson, 1993) through the action of the actin filaments and, in some species, of the microtubules (Sato et al., 2001). In *B. cycloptera*, the microtubules are also involved in the formation, and the maintenance of integrity, of the CCC (Chuong et al., 2006). Therefore, it is highly probable that under prolonged LL, the cytoskeleton directs the movement of chloroplasts to the distal part of the cell in order to enhance light capture; thus, the whole CCC is displaced. Since this process implies the movement of a complex cytoplasmic structure of chloroplasts, mitochondria, and peroxisomes, it is possible that only exposure to LL during development, or over long periods of time, may cause displacement of the CCC, rather than during short-term exposure to LL. No changes in the position of the CCC were observed in normal light/dark cycles; the shift of the CCC to the periphery of the cell occurs within 1 week (J. Park and G. Edwards, unpublished data), but the time course has not been determined.

The relative levels of peptides in M leaves after LL treatment were maintained near preexisting ML growth levels for a number of photosynthetic proteins. Peptide levels in LL-treated leaves, including Rubisco SSU and LSU, PPDK, ALA-AT, mASP-AT, αNAD-ME, AGPase LSU, and GDC-P, were retained at 70% or higher compared with ML-grown leaves, while levels of two mitochondrial peptides, αNAD-ME and mASP-AT, increased under LL treatment. Peptides for PEPC, cASP-AT, and SHMT decreased to approximately 40% to 50% under LL treatment. For a number of enzymes, transcript levels under LL treatment were similar to those of ML-grown leaves. The most noticeable decreases were in transcripts of *Rubisco SSU* (approximately 30%) and *PEPC*, *cASP-AT*, and *ALA-AT* (40% to 60% of levels under ML growth conditions). The results indicate that despite being treated to prolonged treatment with very LL (20 PPFD), there is a decreased investment in Rubisco and PEPC. Since light is limiting, assimilatory power will be rate limiting rather than capacity for carbon assimilation. Thus, a decrease in levels of the carboxylases would prevent excess investment in these enzymes and may coordinate down-regulation of the C_4 and C_3 cycles. Under LL, the pool of C_4 acids that is generated in the C_4 cycle is expected to be low; if increasing levels of αNAD-ME and mASP-AT correspond to an up-regulation of the decarboxylation phase, it may increase the efficiency of utilizing C_4 acids as donors to Rubisco under LL. Since, in the LL treatment, light harvesting is expected to be limiting, the drop in chlorophyll content was unexpected, suggesting an inability of light harvesting to acclimate to such LL levels. In shade-adapted plants, there is normally an increase in light-harvesting chlorophyll (Tazoe et al., 2006).

In order to test the function of LL-treated plants, the response of CO_2 fixation to varying light and CO_2 was analyzed. Gas-exchange analysis shows that M leaves of *B. sinuspersici* from ML growth conditions show a response to variable light intensities and atmospheric CO_2 levels typical for single-cell and Kranz C_4 species (Fig. 8; Edwards and Walker, 1983; Voznesenskaya et al., 2001, 2002; Edwards et al., 2007), characterized by low CO_2 compensation points and photosynthesis being saturated at nearly atmospheric levels of CO_2.

The LL-treated plants showed strong acclimation and a shade-type response (Bjorkman et al., 1972; Boardman, 1977; Tazoe et al., 2006) to varying light by having a much lower light compensation point, photosynthesis being saturated by relatively low light, and light-saturated rates of photosynthesis being much lower than in leaves of ML-grown plants. Also, CO_2 response curves showed that the shade-adapted plants have a much lower CO_2-saturated rate of photosynthesis than ML-grown plants. The CO_2- and light-saturated rates of photosynthesis in plants grown under ML were about 6-fold higher than in plants exposed to LL treatment. It is uncertain what is limiting maximum photosynthesis in leaves from the LL treatment, since most photosynthetic enzymes were retained at levels of 70% or more of those of ML-grown leaves; however, PEPC levels dropped to 40% of those of ML-grown plants. There might be limitations due to reductions in the components of photochemistry or the function of the C_4 cycle, or there might be biophysical limits due to the rearrangement of the CCC.

It is difficult to precisely measure the CO_2 compensation point on branches due to the contribution from dark-type respiration, especially in the shade-acclimated plants having low photosynthetic rates. Nevertheless, the CO_2 compensation points are C_4 like, and the shade-acclimated (LL) plants maintained a reduced CO_2 compensation point similar to plants grown under ML conditions, with little or no sensitivity of photosynthesis to oxygen. This indicates the LL-treated plants maintain physiological characteristics of C_4-type photo-

synthesis; therefore, the integrity and function of the CCC appears to be maintained even though it is shifted toward the periphery of the cell.

There was a shift in the δ ^{13}C values from −17.4‰ in plants grown under ML to −20.0‰ in plants transferred to LL. This could reflect increased leakage of CO_2 being delivered by the C_4 cycle to the cytoplasmic compartment containing Rubisco during photosynthesis under LL. It is known that C_4 plants have increased discrimination against fixing $^{13}CO_2$ under LL, indicative of increased leakage (Henderson et al., 1992; Kubasek et al., 2007). While C_4 values have been reported in M leaves of *B. sinuspersici* grown under ML (Voznesenskaya et al., 2002), in greenhouse-grown plants values ranging from −15.5‰ to −21.1‰ (with the latest developing leaves being most negative) have been reported in *B. cycloptera* (Freitag and Stichler, 2002). These results suggested that the more negative values might be attributed to LL conditions. Also, in the Kranz-type C_4 plant *Amaranthus cruentus*, δ ^{13}C values were more negative in LL-grown leaves (−19.3‰) than in leaves grown in higher light (−16.0‰; Tazoe et al., 2006). Alternatively, the more negative values of LL-treated plants may be related to the shifting of the CCC from the center to the periphery of the cell if it allowed more CO_2 leakage from this compartment. On the other hand, there was a decrease in the ratio of PEPC to Rubisco (based on results from western blots) in the LL-treated plants, which could favor increased donation of CO_2 from C_4 acids to Rubisco (von Caemmerer et al., 1997). Dark respiration may also contribute to more negative isotope values of biomass (Henderson et al., 1992), although shade-adapted leaves tend to have reduced rates of dark respiration (Fig. 8; Bjorkman et al., 1972).

Effects of D Treatment

The anatomy of branches that were enclosed in D for 1 month is, in general, similar to that under ML growth conditions, except that chlorenchyma cells in YB and YT that formed during D treatment are more irregular in shape than those of ML- and LL-grown plants. In D-treated branches, the chlorenchyma cells had no starch, which is expected due to the lack of photosynthesis and the maintenance of the tissue being dependent on importing photosynthate from branches exposed to light (Fig. 3).

M leaves that formed under ML and were then exposed for 1 month to D had no change in structure of the chlorenchyma or in the position of the CCC in the cell, as viewed by light microscopy (Fig. 3, M and N), in contrast to the shift in the CCC to the periphery of the cell in LL-treated leaves (Fig. 2, M and N). However, after treatment for 1 month in prolonged D, the chloroplasts in the CCC were more loosely arranged compared with those in M leaves that remained under ML conditions, suggesting that there is either a loosening of the interaction between the CCC and the cytoskeleton or a decrease in cytoskeleton proteins. After D treatment, the water content of M leaves (as a percentage of fresh mass) and soluble protein per fresh mass were similar to those of leaves growing under ML. Following D treatment, the chlorophyll content per fresh mass was more than doubled (Table I). This indicates that leaves exposed to continuous D actually synthesize more chlorophyll, in contrast to LL treatment, in which there was a marked decrease in chlorophyll content.

The δ ^{13}C value of M leaves became more negative following D treatment, which could occur due to nonphotosynthetic reasons, which are not well defined but include fractionation occurring during respiration (Henderson et al., 1992; Kubasek et al., 2007). With respect to photosynthetic peptides, levels in D-treated M leaves showed a remarkable stability for the retention of photosynthetic enzymes. The levels were similar to those in M leaves under ML for most proteins, including Rubisco LSU and SSU, GDC-P, AGPase LSU, and all C_4 photosynthesis peptides examined, except for PEPC, SHMT, and ALA-AT. PEPC and SHMT levels were 30% to 40% of the levels under ML growth, while ALA-AT was most reduced, to only 5% of that under ML growth conditions. There was a large drop in

Table II. *Sequences of the oligonucleotide primers used for real-time PCR*

In the last column, the length of the product (Prod.; in base pairs) amplified by the corresponding primers is specified.

Gene	Forward Primer	Reverse Primer	Prod.
Rubisco SSU	5′-CGAGACTCTTTCTTACCTTCCACCTC-3′	5′-GTCCAGTAGCGTCCATCATAGTACC-3′	168
CAB	5′-GAAATCCTTGGAGAGGGAAGAATCAC-3′	5′-AGGGAATTCACCAGTGAGGTAAGATG-3′	153
cASP-AT	5′-TGCTAGAGGTACACCTGGAGACTGG-3′	5′-CTCAAACCAGCCATGCTTATCCTC-3′	153
PEPC	5′-GCTTTAGGACATTGCAGCGGTATG-3′	5′-GCTCCTTACGAACAACAGAGCGGTA-3′	147
mASP-AT	5′-CTTCCAATGGGTGGCAGTAACCAC-3′	5′-CGACATGCTCCAGTACCAGACAGAG-3′	123
GO	5′-GGTCGTATTCCTGTGTTCTTGGATG-3′	5′-CATCATCTGCAGGACCTTCCTAAC-3′	159
AGPase LSU	5′-CTGCCAGATTTCTGCCTCCTACAA-3′	5′-CTGAAGCTCAACACCGGACTCTAATC-3′	146
PPDK	5′-GGTAAGGAATGAAACTAGCCCAGAGG-3′	5′-GATCTCAGAGCACCCTGAAACACAAC-3′	145
αNAD-ME	5′-ACCAATGCCTTGGATCCCTAGATC-3′	5′-TAGCTCTGCTGATCGTGGAGAAATG-3′	130
βNAD-ME	5′-GAGACCTCACAGCAGAAGTTGCAG-3′	5′-GAGAGGGCTGTAGACTGGAAACCAC-3′	167
ALA-AT	5′-GCAGAGGGAGCCATGTACCTATTTC-3′	5′-GACGACAACGATTCCAGTCTCTTG-3′	135
GDC-P	5′-CTGAGATTGAGAATGGGAAAGCTGA-3′	5′-GGAAGAAGGGTGCAGACCAAGTTC-3′	217
Elongation factor 1	5′-GCTGTTAAGGATCTCAAGCGTGGT-3′	5′-GAGATGTGTGGCAATCCAACACTG-3′	154

transcripts of *PEPC* and *ALA-AT* during D treatment, indicating that light is required to maintain their transcript levels; this drop in transcripts in the D may limit peptide synthesis and contribute to the drop in levels of the respective proteins. Despite a large decrease in *PPDK* transcripts in the D treatment, the PPDK protein level was 90% of that of ML leaves, suggesting high stability. Following D treatment of M leaves, the ratio of Rubisco (LSU and SSU) to PEPC was about 3-fold higher than that in leaves grown under ML.

B. sinuspersici young and intermediate leaves that develop in D form a pre-CCC, with chloroplasts aggregated near the nucleus and other chloroplasts isolated in the periphery of the cell (Fig. 3). This indicates that intracellular development of two cytoplasmic domains can occur in D. Also, cotyledons of D-grown seedlings of *B. sinuspersici* develop a pre-CCC (E. Voznesenskaya, N. Koteyeva, and G.E. Edwards, unpublished data). Studies on development in amaranth also indicate that morphologically distinguishable Kranz anatomy develops in cotyledons grown in complete D (Wang et al., 1993).

CONCLUSION

In *Bienertia*, there are developmental differences in patterns of photosynthetic gene expression and peptide levels. This indicates a level of complexity with independent regulation of C_4 gene expression. For most of the photosynthetic genes analyzed, there tends to be a close relationship between mRNA levels and the accumulation of peptides during leaf development under ML growth conditions, including Rubisco SSU and six C_4 cycle enzymes, suggesting some control of peptide synthesis at the transcriptional level. An exception was *AGPase LSU*, in which transcript levels were high early in development but peptide levels gradually increased during development, suggestive of posttranscriptional control. Transcriptional control could be a primary means of regulating synthesis of the mitochondrial enzymes αNAD-ME, βNAD-ME, mASP-AT, GDC-P, and SHMT, since there is one type of mitochondrion that is located in the CCC (Voznesenskaya et al., 2002). Also, PEPC, which is located throughout the cytosol, may be controlled by transcript levels, as well as the cytosolic enzymes ALA-AT and cASP-AT. However, for the chloroplastic genes analyzed, *AGPase LSU* and *SSU*, *Rubisco SSU*, and *PPDK*, posttranscriptional regulation is expected (e.g. by mRNA targeting, regulation of translation, or selective mRNA degradation), since, in M leaves, PPDK is selectively localized in the peripheral chloroplasts, while Rubisco and AGPase are selectively localized in chloroplasts in the CCC.

As in Kranz-type species, in the single-cell C_4 species of *Bienertia* there is a progressive developmental transition for the specialized functions of C_4 photosynthesis. Once C_4 is developed in M leaves in *B. sinuspersici*, the cytoplasmic domains are very stable. Only prolonged exposure to very low light was found to cause a structural change with a shift in the position of the CCC. This work shows the remarkable stability of the two cytoplasmic domains under extremes of D and LL. Further studies are needed to determine similarities and differences in mechanisms controlling chloroplast differentiation and the expression of the C_4 system in *B. sinuspersici* compared with Kranz-type C_4 plants.

MATERIALS AND METHODS

Plant Material and Growth Conditions

The species used in the study was *Bienertia sinuspersici* (seeds were kindly provided by Dr. Abdulrahman Alsirhan). Plants were grown in a growth chamber (model GC-16; Enconair Ecological Chambers) under ML, approximately 400 μmol quanta m^{-2} s^{-1}, with a 14/10-h light/dark photoperiod and 25°C/15°C day/night temperature regime, atmospheric CO_2, and 50% relative humidity. Plants were grown in commercial potting soil in 2-L pots (one plant per pot). Plants were watered once weekly with 20:20:20 Peters Professional fertilizer (1 g L^{-1} water) and a salt solution (150 mM NaCl) and otherwise with water alone. The lights in the chamber were programmed to come on and off gradually through a stepwise increase or decrease over a 2-h period at the beginning and end of the photoperiod, respectively. Plants that were 2 to 3 months old were used for this study.

To study the effect of long-term exposure to D, part of the vegetative tissue from the bushy-type growth was covered and completely protected from light, while the remainder of the plant remained under ML growth conditions. Aluminum foil was used to construct over part of the lateral branches a tent-like structure that was sealed to the bottom of the chamber floor (which protected the plant from light, while the chamber design provided aeration from the floor). After 1 month, leaves were sampled from the D treatment and analyzed (called D-treated plants). By marking stem tissue with adhesive labels, any new growth could be distinguished from leaves existing when the treatment began. Young and intermediate leaves were collected from new growth that occurred in the D, while M leaves were collected from leaves that were already mature prior to D exposure.

To study the effects of exposure to extremely LL, a group of plants were transferred and maintained for 1 month in a growth chamber with the same photoperiod and temperature regime, except that the daily level of light was 20 μmol quanta m^{-2} s^{-1} (designated as LL treatment). Again, by marking stem tissue with adhesive labels, new growth could be distinguished from leaves existing when the treatment began. Young and intermediate leaves were collected from new growth that occurred under LL, while M leaves were collected from leaves that were already mature prior to LL exposure.

For protein and RNA analyses, leaf samples were taken and immediately frozen in liquid N_2 and stored at −80°C. In all cases, samples were collected around noon.

Gas-Exchange Analysis

Rates of photosynthesis were measured with an LCpro+ portable infrared CO_2 gas analyzer (ADC Bio Scientific) at varying light intensities and CO_2 concentrations. Photosynthetic rates were expressed per unit of leaf area. A branch of the plant was placed inside the conifer chamber with conditions of 1,000 μmol quanta m^{-2} s^{-1}, 25°C, 340 μbar CO_2, and 12 mbar vapor pressure until a steady-state rate of photosynthesis was achieved. Light response measurements were made while decreasing the PPFD from a maximum of 1,300 to 0 μmol quanta m^{-2} s^{-1} (with 4-min intervals between measurements) and then with increasing PPFD from 0 to 1,300 μmol quanta m^{-2} s^{-1} (with 10-min intervals between measurements). There was no significant difference between the curves generated, whether the sequence was from ML to LL followed by LL to ML or vice versa. The response rates of photosynthesis to varying ambient levels of CO_2 were determined by gradually decreasing external CO_2 concentrations from ambient CO_2 (approximately 340 μbar) to approximately 5 μbar CO_2. This was followed by gradually increasing the CO_2 level from 5 to 927 μbar CO_2 and then decreasing the level to 340 μbar.

Protein Extraction

Total protein from the different samples was extracted using a buffer containing 100 mM Tris-HCl, pH 7.5, 1 mM EDTA, 10 mM $MgCl_2$, 15 mM

β-mercaptoethanol, 20% (v/v) glycerol, 1 mM phenylmethylsulfonyl fluoride, 10 μg mL^{-1} leupeptin, 10 μg mL^{-1} chymostatin, and 10 μL of protease inhibitor cocktail (Sigma) per milliliter of extraction buffer. The samples were ground completely in a cold mortar and centrifuged at 10,000*g* for 10 min at 4°C. The supernatant fractions from crude extracts were used for protein measurement or diluted in 0.25 M Tris-HCl, pH 7.5, 2% (w/v) SDS, 0.5% (v/v) β-mercaptoethanol, and 0.1% (v/v) bromphenol blue and boiled for 2 min for SDS-PAGE. Protein concentration was determined by the method of Bradford (1976) using the Bio-Rad protein assay reagent (and bovine serum albumin as a standard).

Chlorophyll Assay

Chlorophyll was extracted in 80% (v/v) acetone and analyzed as described by Lichtenthaler (1987).

Gel Electrophoresis

SDS-PAGE was performed on 12.5% (w/v) polyacrylamide gels according to Laemmli (1970). Proteins were visualized with Coomassie Brilliant Blue or electroblotted onto a nitrocellulose membrane for immunoblotting according to Burnette (1981). Bound antibodies were located by linking to alkaline phosphatase-conjugated goat anti-rabbit IgG or anti-mouse IgG (for actin and tubulin) according to the manufacturer's instructions (Bio-Rad). The antibodies used for detection, with dilutions in parentheses, were as follows: anti-*Amaranthus viridis* PEPC (1:200; Colombo et al., 1998), serum against the α-subunit of NAD-ME from *Amaranthus hypochondriacus* (1:5,000; Long et al., 1994), anti-*Zea mays* PPDK (1:10,000; courtesy of Dr. T. Sugiyama), anti-*Panicum mileaceum* ALA-AT (specific for C_4 isoform-ALAAT-2 in the NAD-ME C_4 species *P. milaceum*; Son et al., 1991), cASP-AT (1:3,000; courtesy of Dr. M. Taniguchi; Sentoku et al., 2000), anti-*Eleusine coracana* mASP-AT (1:2,500; specific for the mitochondrial isoform in the NAD-ME species *E. coracana*; Taniguchi and Sugiyama, 1990), anti-SHMT (1:1,000; courtesy of Dr. H. Bauwe), anti-GDC-P (1:1,000; courtesy of Dr. D. Oliver), anti-spinach (*Spinacia oleracea*) Rubisco LSU (1:10,000; courtesy of Dr. B. McFadden), anti-*A. hypochondriacus* Rubisco SSU (1:5,000; courtesy of Dr. J. Berry), anti-spinach large subunit of AGPase (1:1,000; courtesy of Dr. T. Okita), anti-chicken gizzard skeletal actin (1:3,000; clone C4; ICN Biomedicals), and anti-bovine β-tubulin (1:3,000; T4026; Sigma-Aldrich). The molecular masses of the polypeptides were estimated from a plot of the log of the molecular masses of marker standards versus migration distance. The intensities of bands in western blots were semiquantified with image-analysis software and expressed relative to levels in the M leaf. For most proteins, there was an increase in band intensity during leaf development. To guard against overloading, based on initial staining patterns with the dilutions of antibodies selected, 5 μg of soluble protein was added per lane for Rubisco LSU and 20 μg of soluble protein was added per lane for other enzymes, which was sufficient for detection of the lowest levels.

Light Microscopy and Polysaccharide Staining

Samples were taken from fresh leaves for light microscopy and starch analysis and fixed at 4°C in 2% (v/v) paraformaldehyde and 1.25% (v/v) glutaraldehyde in 0.05 M PIPES buffer, pH 7.2. The samples were dehydrated with a graded ethanol series and embedded in LR White (Electron Microscopy Sciences) acrylic resin. Cross sections, 0.8 to 1 μm thick, were made on a Reichert Ultracut R ultramicrotome (Reichert-Jung) and placed onto gelatin-coated slides for light microscopy; sections were stained with 1% (w/v) toluidine blue O in 1% (w/v) $Na_2B_4O_7$. For polysaccharides, staining sections, 0.8 to 1 μm thick, were incubated in periodic acid (1%, w/v) for 30 min, washed, and then incubated with Schiff's reagent (Sigma) for 1 h. After rinsing, the sections were ready for observation with light microscopy. Images were acquired through an Olympus BH-2 light microscope using a Jenoptik ProgRes C12plus digital camera.

RNA Isolation and RT-PCR

Total RNA from different samples of *B. sinuspersici* was isolated from 60 mg of tissue using the SV RNA Isolation System (Promega), which includes DNase treatment to eliminate contamination with genomic DNA, according to the manufacturer's instructions. The integrity of the RNA was verified by agarose electrophoresis. The quantity and purity of the RNA were determined spectrophotometrically according to the method described by Sambrook et al. (1989). First-strand cDNA was synthesized with Moloney murine leukemia virus reverse transcriptase following the manufacturer's instructions (Promega) and using 2 μg of RNA and oligo(dT).

QRT-PCR

Relative expression was determined by performing QRT-PCR on 96-well plates and amplified in an automated fluorometer (ABI PRISM 7700 Sequence Detection System; Applied Biosystems) using the intercalation dye SYBR Green I (Invitrogen) as a fluorescent reporter, with 2.5 mM $MgCl_2$, 0.5 μM of each primer, and 0.04 units μL^{-1} GoTaq (Promega). PCR primers were designed with the aid of the Web-based program primer3 (http://frodo.wi.mit.edu) to produce amplicons of 130 to 217 bp in size (Table II) based on *B. sinuspersici* cDNA sequences obtained in the laboratory (data not shown). A 10-fold dilution of cDNA, obtained as described above, was used as a template. Cycling parameters were as follows: initial denaturation at 94°C for 2 min; 40 cycles of 94°C for 10 s, 58°C for 15 s, and 72°C for 1 min; and finally 72°C for 10 min. Melting curves for each PCR were determined by measuring the decrease of fluorescence with increasing temperature (from 60°C to 98°C). The specificity of the PCRs was confirmed by melting curve analysis using the software as well as by agarose gel electrophoresis of the products. Threshold values were determined automatically using ABI PRISM 7000 software, and the resulting C_t values (for threshold cycle for a given gene amplification) were generated for each of three sample replicates. Relative gene expression was calculated using the comparative $2^{-\Delta\Delta CT}$ method (Livak and Schmittgen, 2001) with elongation factor 1 as a reference gene. For each primer set, at least two independent RNA samples were tested in triplicate for a total of six replicates per gene per sample.

Carbon Isotope Composition and δ ^{13}C Values

δ ^{13}C values were determined at Washington State University on leaf samples taken from plants using a standard procedure relative to Pee Dee Belemnite limestone as the carbon isotope standard (Bender et al., 1973). Plant samples were dried at 80°C for 24 h and milled to a fine powder, and then 1 to 2 mg was placed into a tin capsule and combusted in a Eurovector elemental analyzer. The resulting N_2 and CO_2 gases were separated by gas chromatography and admitted into the inlet of a Micromass Isoprime isotope ratio mass spectrometer for the determination of $^{13}C/^{12}C$ ratios. δ ^{13}C was determined where $\delta = 1{,}000 \times (R_{sample}/R_{standard}) - 1‰$. For the determination of carbon isotope composition during development (YB, YT, IB, and IT), up to 25 to 35 leaf sections were taken for each stage, combined for isotope analysis, and replicated twice.

ACKNOWLEDGMENTS

M.V.L. and C.S.A. are members of the Researcher Career of Consejo Nacional de Investigaciones Científicas y Técnicas. We thank the Franceschi Microscopy and Imaging Center of Washington State University for the use of facilities and for staff assistance, and we thank C. Cody for plant growth management.

Received June 3, 2008; accepted July 21, 2008; published July 30, 2008.

LITERATURE CITED

Akhani H, Barroca J, Koteeva N, Voznesenskaya EV, Franceschi VR, Edwards GE, Ghaffari SM, Ziegler H (2005) *Bienertia sinuspersici* (Chenopodiaceae): a new species from southwest Asia and discovery of a third terrestrial C_4 plant without Kranz anatomy. Syst Bot **30:** 290–301

Akhani H, Trimborn P, Ziegler H (1997) Photosynthetic pathways in Chenopodiaceae from Africa, Asia and Europe with their ecological, phytogeographical and taxonomical importance. Plant Syst Evol **206:** 187–221

Bender MM, Rouhani I, Vines HH, Black CC Jr (1973) $^{13}C/^{12}C$ ratio changes in Crassulacean acid metabolism plants. Plant Physiol **52:** 427–430

Bjorkman O, Boardman NK, Anderson JM, Thorne SW, Goodchild DJ, Pyliotis NA (1972) Effect of light intensity during growth of *Atriplex patula* on the capacity of photosynthetic reactions, chloroplast components and structure. Carnegie Inst Washington Year Book **71:** 115–135

Boardman NK (1977) Comparative photosynthesis of sun and shade plants. Annu Rev Plant Physiol **28:** 355–357

Bradford MM (1976) A rapid and sensitive method for the quantitation of microgram quantities of protein utilizing the principle of protein-dye binding. Anal Biochem **72:** 248–252

Burnette WN (1981) ''Western blotting'': electrophoretic transfer of proteins from sodium dodecyl sulfate-polyacrylamide gels to unmodified nitrocellulose and radiographic detection with antibody and radioiodinated protein A. Anal Biochem **112:** 195–203

Cahoon AB, Takacs EM, Sharpe RM, Stern DB (2008) Nuclear, chloroplast, and mitochondrial transcript abundance along a maize leaf developmental gradient. Plant Mol Biol **66:** 33–46

Cerling TE (1999) Paleorecords of C_4 plants and ecosystems. *In* RF Sage, RK Monson, eds, C_4 Plant Biology. Academic Press, San Diego, pp 133–172

Chuong SDX, Franceschi VR, Edwards GE (2006) The cytoskeleton maintains organelle partitioning required for single-cell C_4 photosynthesis in Chenopodiaceae species. Plant Cell **18:** 2207–2223

Colombo SL, Andreo CS, Chollet R (1998) The interaction of shikimic acid and protein phosphorylation with PEP carboxylase from the C_4 dicot *Amaranthus viridis*. Phytochemistry **48:** 55–59

Edwards GE, Franceschi VR, Voznesenskaya EV (2004) Single-cell C_4 photosynthesis versus the dual-cell (Kranz) paradigm. Annu Rev Plant Biol **55:** 173–196

Edwards GE, Voznesenskaya E, Smith M, Koteyeva N, Park Y, Park JH, Kiirats O, Okita TW, Chuong SDX (2007) Breaking the Kranz paradigm in terrestrial C_4 plants: does it hold promise for C_4 rice? *In* JE Sheehy, PL Mitchell, B Hardy, eds, Charting New Pathways to C_4 Rice. International Rice Research Institute, Makati City, Philippines, pp 249–273

Edwards GE, Walker DA (1983) C_3, C_4: Mechanisms, and Cellular and Environmental Regulation of Photosynthesis. Blackwell Scientific, London

Freitag H, Stichler W (2002) *Bienertia cycloptera* Bunge ex Boiss., Chenopodiaceae, another C_4 plant without Kranz tissues. Plant Biol **4:** 121–131

Henderson SA, von Caemmerer S, Farquhar GD (1992) Short-term measurements of carbon isotope discrimination in several C_4-species. Aust J Plant Physiol **19:** 263–285

Kandasamy MK, Meagher RB (1999) Actin-organelle interaction: association with chloroplast in Arabidopsis leaf mesophyll cells. Cell Motil Cytoskeleton **44:** 110–118

Kubasek J, Setlik J, Dwyer S, Santrucek J (2007) Light and growth temperature alter carbon isotope discrimination and estimated bundle sheath leakiness in C_4 grasses and dicots. Photosynth Res **91:** 47–58

Laemmli UK (1970) Cleavage of structural proteins during the assembly of the head of bacteriophage T_4. Nature **227:** 680–685

Langdale JA, Nelson T (1991) Spatial regulation of photosynthetic development in C_4 plants. Trends Genet **7:** 191–196

Langdale JA, Zelitch I, Miller E, Nelson T (1988) Cell position and light influence C_4 versus C_3 patterns of photosynthetic gene expression in developing maize. EMBO J **7:** 3643–3651

Lichtenthaler HK (1987) Chlorophylls and carotenoids: pigments of photosynthetic biomembranes. Methods Enzymol **148:** 350–382

Livak KJ, Schmittgen TD (2001) Analysis of relative gene expression data using real-time quantitative PCR and the $2^{-\Delta\Delta CT}$. Methods **25:** 402–408

Long JJ, Berry JO (1996) Tissue-specific and light-mediated expression of the C_4 photosynthetic NAD-dependent malic enzyme of amaranth mitochondria. Plant Physiol **112:** 473–482

Long JJ, Wang JL, Berry JO (1994) Cloning and analysis of the C_4 NAD-dependent malic enzyme of amaranth mitochondria. J Biol Chem **269:** 2827–2833

Patel M, Berry JO (2008) Rubisco gene expression in C_4 plants. J Exp Bot **59:** 1625–1634

Patel M, Corey AC, Yin LP, Ali S, Taylor WC, Berry JO (2004) Untranslated regions from C_4 amaranth AhRbcS1 mRNAs confer translational enhancement and preferential bundle sheath cell expression in transgenic C_4 *Flaveria bidentis*. Plant Physiol **136:** 3550–3561

Sage RF, Monson RK (1999) C_4 Plant Biology. Academic Press, San Diego

Sambrook J, Fritsch EF, Maniatis T (1989) Extraction, purification, and analysis of messenger RNA from eukaryotic cells. *In* C Nolan, ed, Molecular Cloning: A Laboratory Manual. Cold Spring Harbor Laboratory Press, Cold Spring Harbor, NY, pp 7.3–7.84

Sato Y, Wada M, Hashimoto T (2001) Choice of tracks, microtubules and/or actin filaments for chloroplast photo-movement is differentially controlled by phytochrome and blue light receptor. J Cell Sci **114:** 269–279

Sentoku N, Taniguchi M, Sugiyama T, Ishimaru K, Ohsugi R, Takaiwa F, Toki S (2000) Analysis of the transgenic tobacco plants expressing *Panicum miliaceum* aspartate aminotransferase genes. Plant Cell Rep **19:** 598–603

Sheahan MB, Rose RJ, McCurdy DW (2004) Organelle inheritance in plant cell division: the actin cytoskeleton is required for unbiased inheritance of chloroplasts, mitochondria and endoplasmic reticulum in dividing protoplasts. Plant J **3:** 379–390

Sheen J (1999) C_4 gene expression. Annu Rev Plant Physiol Plant Mol Biol **50:** 187–217

Sheen JY, Bogorad L (1987) Differential expression of C_4 pathway genes in mesophyll and bundle sheath cells of greening maize leaves. J Biol Chem **262:** 11726–11730

Son D, Jo J, Sugiyama T (1991) Purification and characterization of alanine aminotransferase from *Panicum miliaceum* leaves. Arch Biochem Biophys **289:** 262–266

Taniguchi M, Sugiyama T (1990) Aspartate aminotransferase from *Eleusine coracana*, a C_4 plant: purification, characterization, and preparation of antibody. Arch Biochem Biophys **282:** 427–432

Tazoe Y, Noguchi K, Terashima I (2006) Effects of growth light and nitrogen nutrition on the organization of the photosynthetic apparatus in leaves of a C_4 plant, *Amaranthus cruentus*. Plant Cell Environ **29:** 691–700

von Caemmerer S, Millgate A, Farquhar GD, Furbank RT (1997) Reduction of ribulose-1,5-bisphosphate carboxylase/oxygenase by antisense RNA in the C_4 plant *Flaveria bidentis* leads to reduced assimilation rates and increased carbon isotope discrimination. Plant Physiol **113:** 469–477

Voznesenskaya EV, Edwards GE, Kiirats O, Artyusheva EG, Franceschi VR (2003) Development of biochemical specialization and organelle partitioning in the single-cell C_4 system in leaves of *Borszczowia aralocaspica* (Chenopodiaceae). Am J Bot **90:** 1669–1680

Voznesenskaya EV, Franceschi VR, Kiirats O, Artyusheva EG, Freitag H, Edwards GE (2002) Proof of C_4 photosynthesis without Kranz anatomy in *Bienertia cycloptera* (Chenopodiaceae). Plant J **31:** 649–662

Voznesenskaya EV, Franceschi VR, Kiirats O, Freitag H, Edwards GE (2001) Kranz anatomy is not essential for terrestrial C_4 plant photosynthesis. Nature **414:** 543–546

Voznesenskaya EV, Franceschi VR, Pyankov VI, Edwards GE (1999) Anatomy, chloroplast structure and compartmentation of enzymes relative to photosynthetic mechanisms in leaves and cotyledons of species in the tribe Salsoleae (Chenopodiaceae). J Exp Bot **50:** 1779–1795

Voznesenskaya EV, Koteyeva NK, Choung SD, Akhani H, Edwards GE, Franceschi V (2005) Differentiation of cellular and biochemical features of the single-cell syndrome during leaf development in *Bienertia cycloptera* (Chenopodiaceae). Am J Bot **92:** 1784–1795

Wang JL, Klessig DF, Berry JO (1992) Regulation of C_4 gene expression in developing amaranth leaves. Plant Cell **4:** 173–184

Wang JL, Long JJ, Hotchkiss T, Berry JO (1993) C_4 photosynthetic gene expression in light- and dark-grown amaranth cotyledons. Plant Physiol **102:** 1085–1093

Wang SM, Lue WL, Yu TS, Long JH, Wang CN, Eimert K, Chen J (1998) Characterization of ADG1, an Arabidopsis locus encoding for ADPG pyrophosphorylase small subunit, demonstrates that the presence of the small subunit is required for large subunit stability. Plant J **13:** 63–70

Williamson RE (1993) Organelle movements. Annu Rev Plant Physiol **44:** 181–202